JOURNAL OF SOLID STATE CHEMISTRY **131,** 43–48 (1997)
ARTICLE NO. SC977302

Preparation of $BaTiO_3$ Thin Films Using Glycolate Precursor

H. Nishizawa and M. Katsube

Department of Chemistry, Faculty of Science, Kochi University, Kochi 780, Japan

Received August 15, 1996; in revised form January 28, 1997; accepted January 30, 1997

The translucent grease-like gel was obtained by heating the mixed solution of monohydrated barium hydroxide and titanium isopropoxide in ethylene glycol up to 145°C. The gel consisted of EG (ca. 90%) and residual flake-like microcrystals with a characteristic low-angle X-ray diffraction peak ($d = 1.187$ nm). The thermal decomposition of the gel proceeded through three major stages, viz., (i) evolution of EG ($\sim$200°C), (ii) decomposition of EG moiety in microcrystal to form an amorphous carbonate ($\sim$400°C), and (iii) crystallization of cubic $BaTiO_3$ with a grain size of 10 to 20 nm ($\sim$600°C). Spectroscopic and thermoanalytical techniques were used to characterize the glycolate precursor and the intermediate isolated at various stages. Smooth and transparent $BaTiO_3$ films with 2–3 μm thickness were obtained by painting the gel once on several substrates and heating up to above 600°C. $BaTiO_3$ films prepared were strongly oriented along the (110) plane.

1. INTRODUCTION

$BaTiO_3$ is an important material for the electronics industry (1, 2) and due to its surface sensitivity to gas absorption, applications have been explored in chemical sensors (3–5). For these reasons, a number of methods for the preparation of $BaTiO_3$ thin films such as vacuum evaporation (6), electrodeposition (7), and r.f. sputtering (8) have been proposed. The chemical methods such as sol–gel (9–11) and metal–organic decomposition (MOD) (12, 13) have also been explored. Especially the sol–gel processings have the advantages of using relatively inexpensive and easier to handle reagents and simple equipment. Sol–gel and sol-precipitation techniques are based on the use of these metal–organic precursors and applied to the preparation of crystalline powders and thin films.

Some authors have proposed that the solution-derived metal organic precursors, such as a citrate salt, BaTi $(C_6H_6O_7)_3 6H_2O$ (14), an oxalate salt, $BaTiO(C_2O_4)_2 4H_2O$ (15), and a neodecanoate-based precursor (16), decompose to form a finely divided mixture of $BaCO_3$ and TiO_2, which subsequently reacts to form $BaTiO_3$ on heating at 600–700°C in air. Recently Rajendran and Rao reported the citrate precursor barium bis(citrate)oxotitanate(IV) citrate heptahydrate (17), which decomposes to form not the mixture of $BaCO_3$ and TiO_2 but an oxycarbonate $Ba_2Ti_2O_5CO_3$ as intermediate before the formation of $BaTiO_3$.

Fukushima *et al.* (18) used barium naphtalate and a titanium alkoxide as source materials. A butanol solution of these precursors was spread on a glass or quartz substrate. After evaporation of solvent, a calcination treatment was employed to remove the organics. $BaTiO_3$ films showing interference colors were obtained by calcination above 400°C. Mohallem and Aegerter (19) used barium acetate and titanium isopropoxide for the deposition of thin films by a dipping technique. The films were amorphous up to 550°C. Crystallization to an apparently tetragonal structure occurred after heat treatment at 600°C. In these wet chemical techniques, larger areas with complicated geometries can be coated successfully. But the sol–gel processings for thin film deposition suffer from two limitations: (i) relatively high crystallization temperatures cause reactions with substrates, and (ii) preparation of thick coatings (from 10 to 15 μm) cannot be achieved in a single step.

In the present work, the reaction of barium hydroxide and titanium alkoxide has been examined using ethylene glycol as solvent. The structure of the new glycolate precursor and the reaction path to $BaTiO_3$ are presented. This glycolate precursor has been painted on several kinds of substrates and calcined at relatively low temperatures for preparation of $BaTiO_3$ thin films.

2. EXPERIMENTAL DETAILS

(1) *Preparation of Glycolate Precursor*

Monohydrated barium hydroxide obtained by heating $Ba(OH)_2 8H_2O$ at 200°C in air was dissolved in ethylene glycol $HO(CH_2)_2OH$ under stirring at 80°C for 80 min. Then, titanium isopropoxide $Ti(OC_3H_7)_4$ was added with the Ba/Ti molar ratio of 1. The mixed solution was heated under stirring at a rate of 10°C/min. The solution became turbid at 145°C and a translucent gel was obtained. The gel was maintained at temperatures between 160 and 190°C for 1 h to promote complexation. The gels obtained at temperature T are denoted as G–T (G-160 etc.). The gel was

0022-4596/97 $25.00

separated by centrifuging and washing twice with acetone. This grease-like gel was stable in air.

(2) *Preparation of Thin Film*

The films were obtained by painting the gel on substrates (Pyrex glass, alumina plate, stainless sheet, and Pt sheet) about 0.5 mm thick and heating in air. For $BaTiO_3$ crystallization, the films were heated in air up to temperatures $>600°C$.

(3) *Characterization*

Thermal evolution of the gel was monitored by X-ray diffraction analysis (XRD) using a high temperature Gunier–Lenne camera at a rate of 1.2°C/h. Thermogravimetry and differential analysis (MAC TG-DTA 2000) were also conducted with a heating rate of 10°C/min. Powder X-ray diffraction was recorded on a Rigaku RAD-IIC diffractometer with Cu$K\alpha$ radiation and a graphite monochromometer. FT-IR data were obtained with a JASCO FT/IR-5300 Fourier transformation infrared spectrometer. The infrared pellets were prepared for the samples obtained by heating the gel at above 200°C by using about 0.5 wt % samples in KBr. The gel sample was observed by painting on NACl disk. The morphology of the product was examined with transmission electron microscopy (Philips STEM CM12). Microstructure and composition of the films were observed using SEM and EPMA.

3. RESULTS AND DISCUSSION

(1) *High-Temperature X-Ray Diffraction of Gels*

The most significant feature of X-ray diffraction patterns of the starting gels is that it exhibited a low-angle diffraction peak with high intensity. XRD pattern of G-190 contained some very weak peaks (0.325, 0.2875, 0.235, 0.205 nm) besides a low-angle peak (1.187 nm). This pattern could not be satisfactorily matched with any of the known crystalline phases in the Ba–Ti–O–C–H system. The similar patterns except for the shift of the low-angle peak were observed for the samples obtained by refluxing below 180°C (Fig. 1). The d value of the low-angle peak increased when the refluxing temperature was decreased (1.443 nm at 160°C). A TEM photograph (Fig. 2a) of G-190 ultrasonically dispersed in acetone shows the aggregation of the flake-like crystals.

The thermal evolution of G-190 is shown by the high temperature Guinier–Lenne film up to 700°C (Fig. 3). A very broad low-angle diffraction peak remained up to around 330°C. Then the low-angle peak disappeared and a distinct peak could not be detected. This shows the transformation to the amorphous phase. Subsequently, the crystallization of $BaTiO_3$ occurred at 520°C. The crystal structure was cubic with the lattice constant $a = 0.4005$ nm.

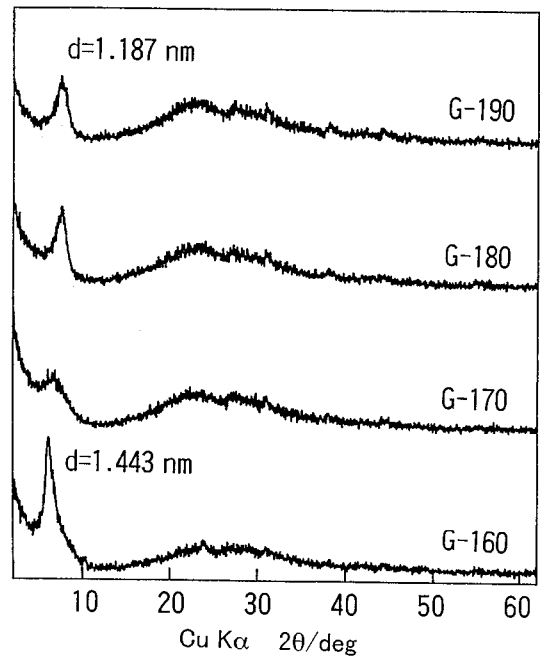

FIG. 1. XRD patterns of the gels precipitated under refluxing at 160 to 190°C.

A TEM photograph (Fig. 2c) of the calcined powders of G-190 at 600°C shows that the grain size of $BaTiO_3$ are in the range of about 10 to 20 nm. This result agrees with that obtained by the study on the particle size dependence of the crystal structure of fine powder $BaTiO_3$ (8), where the cubic phase appears at room temperature below the critical grain size (120 nm).

(2) *TG-DTA of Gels*

Figure 4 shows TG-DTA curves of the gels G-190. Noticeable differences could not be observed on the gels obtained by refluxing above 170°C. The main endothermic peak characterized by an abrupt weight loss, 90% for G-190 and 76% for G-160, occurred below 200°C (Fig. 4a). It was followed by two or three slight weight losses accompanied by exothermic peaks between 200 and 600°C (Fig. 4b). The former is associated to the removal of free ethylene glycol. The latter shows the combustion of organic residuals in crystalline phase up to high temperature. Molecular weights of these organic residuals were evaluated to be in the range from 60 to 66 (62 for ethylene glycol) per 1 mole of $BaTiO_3$.

(3) *FT-IR of Intermediate Phases*

In an attempt to better understand what phases are formed once the volatile component is expelled, an experiment was performed whereby the gel was heated in a furnace at several temperatures up to 700°C for 30 min,

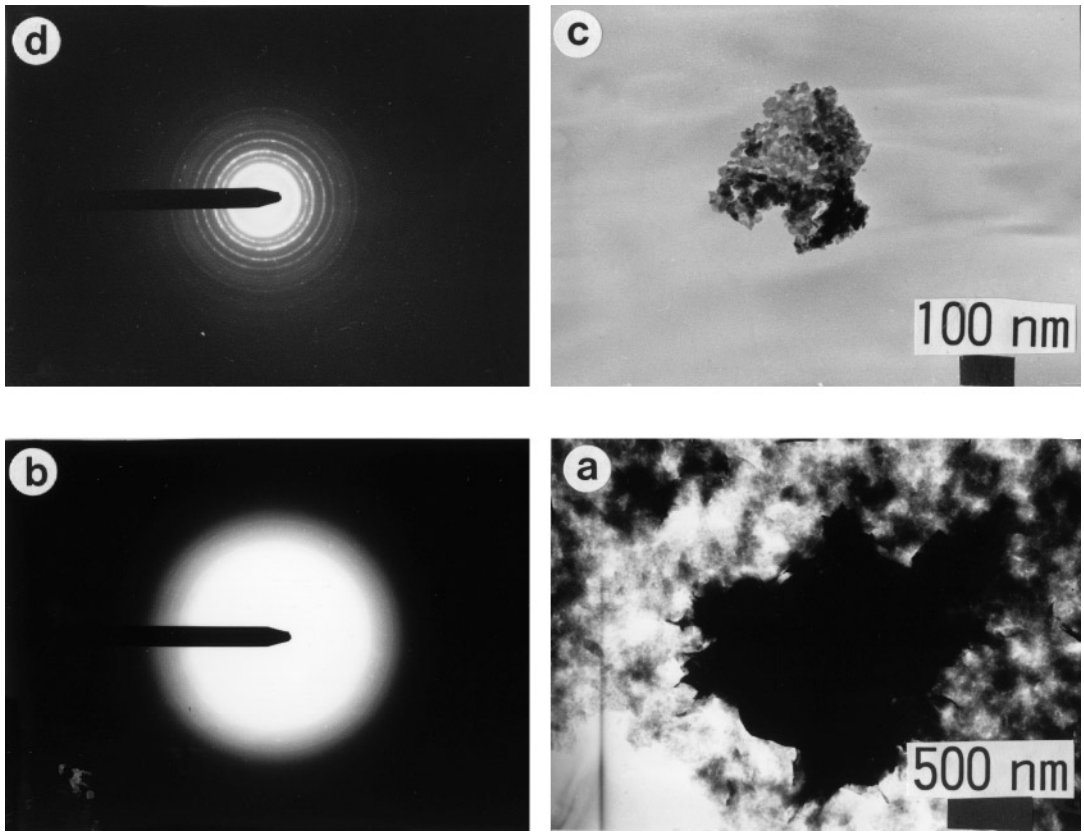

FIG. 2. Transmission electron micrographs and SAD of (a, b) G-190, and (c, d) calcined G-190 at 600°C.

followed by FT-IR analysis. These results are shown in Fig. 5. Except for two bands at 654 and 567 cm^{-1}, FT-IR spectra of G-190 agreed very closely with that of ethylene glycol. It shows that a large amount of absorbed ethylene glycol remains even after several washes with acetone. Absorption bands for the crystalline phase obtained by annealing G-190 at 200°C and neat ethylene glycol are listed in Table 1. The absorption bands of G-190 annealed at 200°C

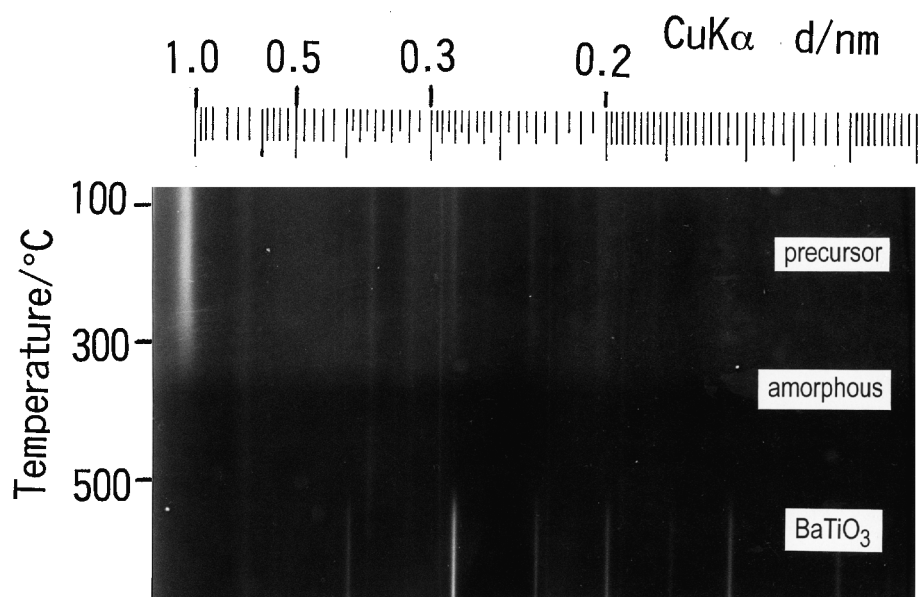

FIG. 3. X-ray powder diffraction pattern of G-190 on heating (Guinier–Lenne camera).

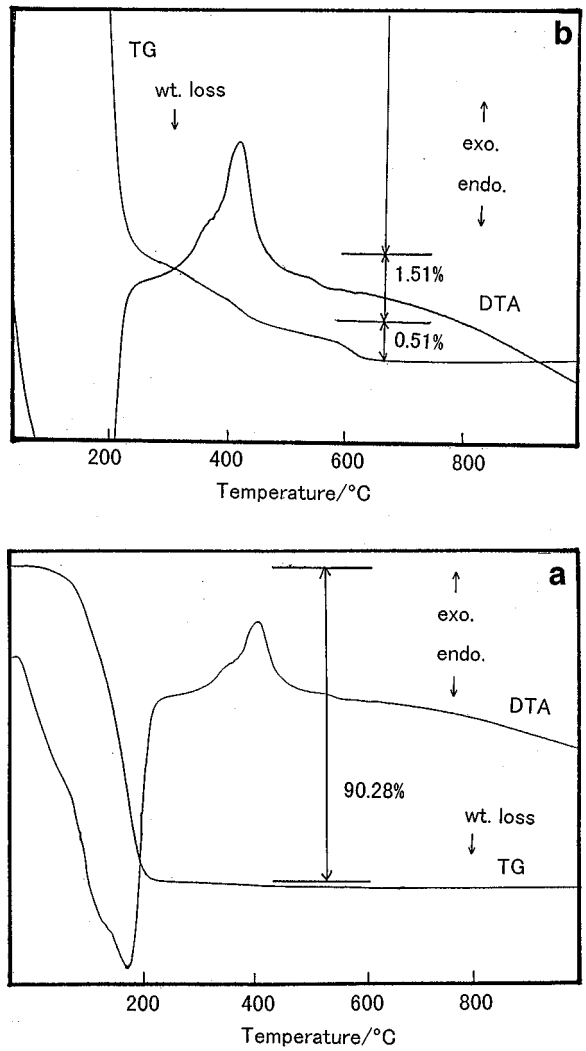

FIG. 4. TG-DTA of G-190 showing (a) evolution of EG from 100 to 200°C and (b) combustion of EG moiety in microcrystal from 200 to 600°C.

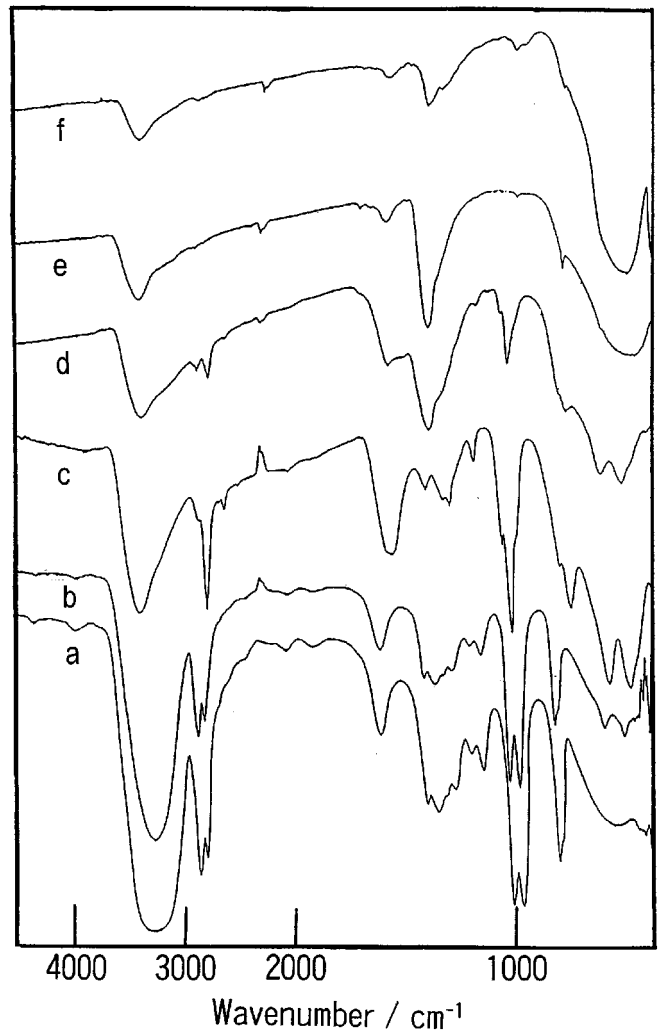

FIG. 5. FT-IR spectra of (a) EG, (b) G-190, and calcined samples at (c) 200, (d) 300, (e) 500, and (f) 600°C.

are very similar to those of ethylene glycol but some bands disappear and shift. The organic residue related to EG is not free in the crystal structure of calcined G-190 because the organic residue was stable beyond the boiling point (198°C) of EG. This means that the crystalline phase with the low-angle XRD peak (1.187 nm) contains organic residue related to EG in the crystal lattice.

The broad band above 3356 cm^{-1} of the O–H stretching vibration in G-190 was shifted to higher wave number in the crystalline phase. In G-190, two peaks in the C–H region appeared at about 2880 and 2946 cm^{-1}. This corresponds roughly to the symmetric and antisymmetric C–H stretching bands of neat ethylene glycol. There appears to be three distinct C–H stretching bands at 2672, 2824, and 2899 cm^{-1} in the crystalline phase. Appearance of the fine structure of ν_{CH} and δ_{CH} implies that glycolate anion cannot move freely in the crystal lattice.

Neat ethylene glycol is characterized by two absorption bands, due to the C–C–O stretching at 1086 and 1043 cm^{-1} which could not be detected in crystalline phase. The presence of bands at around 1100 cm^{-1} and 675–550 cm^{-1} was mentioned recently as being characteristic of the Al–O–C linkage in the case of a barium aluminate glycolate (20). The C–O–Ti bands characteristic of butoxy groups linked to titanium located at 1035, 1085, and 1135 cm^{-1} (21). The disappearance of the EG bands at 1086 and 1043 cm^{-1} corresponding to ν_{C-O} proves that H–O–C bonds have been replaced by Ti–O–C bonds. The three bands at 1057, 1092, 1123, and 664 cm^{-1} in the crystalline phase must be assigned to the C–O–Ti characteristic of ethylene glycoxy groups linked to titanium. Four bands of weak or very weak intensity can be clearly identified on the crystalline phase spectrum, at 1231, 1343, 1373, and 1449 cm^{-1}. This region is diagnostic of the conformation, gauche or trans, of the

TABLE 1
FTIR Bands of EG, G-190, and Calcined Samples

EG (liq) (cm^{-1})	G-190 (cm^{-1})	Calcined samples		
		200°C (cm^{-1})	300°C (cm^{-1})	600°C (cm^{-1})
3356	3356	3424	3422	3430
2946	2946	2899	2926	
2880	2880	2824	2824	
		2672	2674	
			2363	
1651	1651	1630		
		1605	1608	1636
			1435	1454
1458	1458	1449		
1410	1408	1373		
1333	1339	1343		
1256	1256	1231	1225	
1206	1205			
1086	1086	1123	1123	
1043	1042	1092	1090	1082
		1057		
			858	858
883	881	872		
		828	828	
637	654	664	667	
	567	571	575	538

ethyleneoxy, O–CH_2–CH_2–O, groups. The lack of a band at 1322 cm^{-1} was assumed to be diagnostic of ethyleneoxy units in the gauche conformation (22). The bands (571, 463, and 438 cm^{-1}) in the range below 600 cm^{-1} are characteristic of the Ti–O–Ti stretching and bending vibrations.

The crystalline phase obtained by annealing G-190 at 300°C also showed O–H (3422 cm^{-1}), C–H (2926, 2824, and 2674 cm^{-1}), C–O–Ti (1123, 1090, 667 cm^{-1}), and Ti–O–Ti (575, 463, and 438 cm^{-1}) bands. The spectra of this crystalline phase with a low angle XRD peak (1.11 nm) was very similar to that of the precursor phase with a 1.187 nm peak. Thus these two crystalline phases have the same basic structure which is presumed to be interlayered complexes with ethylene glycol. Inoue *et al.* (23, 24) found that the thermal treatment of crystalline aluminum hydroxide in an ethylene glycol medium yielded a novel derivative of boehmite in which the ethylene glycol moiety was incorporated into the boehmite layers. The XRD pattern and IR spectrum suggested that the product has 1.16 nm (020) spacing for a layer structure of boehmite with the ethylene glycol moiety incorporated between the boehmite layers through covalent bonding. The TEM photograph of G-190 (Fig. 2a) shows flake-like crystals with about 100 nm grain size which is characteristic of crystals with layered structure. From these results it was suspected that the space within the titanate layers is "saturated" with ethylene glycol molecules and barium ions.

Increased amorphization of the structure at 400 and 500°C was evidenced by the increased diffuseness and weakening of the Ti–O band at 575 cm^{-1}. The extremely broad bands around 584 cm^{-1} present in the spectra indicated a disordered molecular structure similar to that seen for glasses. The bands due to ethylene glycol completely disappeared and the strong band at 1437 cm^{-1} with weak bands at 858, 1069, 1634, 1750, and 2361 cm^{-1} related to carbonate formation appeared. But the XRD patterns for both of these samples showed no trace of peaks corresponding to crystalline $BaCO_3$. The spectra do not indicate a phase-separated material consisting of crystalline $BaCO_3$ and TiO_2; instead, they indicate the presence of an intermediate carbonate phase in which Ba and Ti cations are randomly distributed. Such carbonate formations have frequently been observed as precursors of $BaTiO_3$ during the alkoxide synthesis process (25).

The absorption bands at 538 and 400 cm^{-1} due to the characteristic peaks of $BaTiO_3$ (26) appeared above 600°C.

(4) *Preparation of Thin Film*

The thin films formed on the Pyrex glass substrate were used for XRD analysis. These results are shown in Fig. 6. The low-angle XRD peak (1.187 nm) of the crystalline phase buried in G-190 was shifted to a little higher angle (1.11 nm) at 300°C. Such transformation occurred also in G-160 (from 1.443 to 1.11 nm) at 200°C. Such shrinkage of the spacing was assumed to be due to evolution of a part of the ethylene glycol moiety in the titanate layer.

The amorphous phase appeared between 400 and 500°C. It followed by the crystallization of cubic $BaTiO_3$ occurs at around 600°C. These changes in G-160 occurred at temperatures lower by about 100°C. The films formed above 500°C for G-160 and 600°C for G-190 showed only the (110) peak of $BaTiO_3$. This means that $BaTiO_3$ films grow with the [110] preferred orientation perpendicular to the substrate surface. Such preferred orientation was observed in the thin films on all substrates used in the present work (Pyrex glass, alumina, stainless steel, and Pt plate). This indicated that the crystal growth of $BaTiO_3$ in films is independent of substrates. The [110] preferred orientation was also observed in the $BaTiO_3$ films deposited by sputtering (13, 27).

By comparing the peak-to-peak height ratios of barium, titanium, and oxygen in the films with those of $BaTiO_3$ single crystal using EPMA, quantitative chemical analysis of the films has been made. The films calcined at 700°C have nearly stoichiometric composition. The mechanical attaching strength of the film to the substrate was high enough to prevent their peeling off when scratched. The films on the glass substrate were smooth and transparent with a refractive index of 2.19. Figure 7 shows a SEM photograph of the thin film (G-190) painted on the stainless steel substrate and calcined at 700°C for 30 min. The $BaTiO_3$ film was

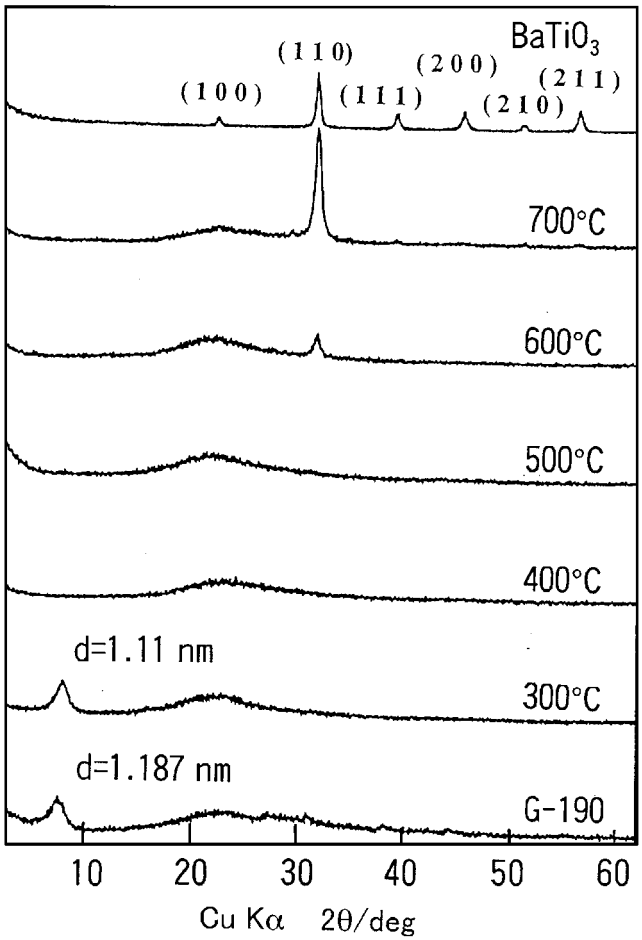

FIG. 6. XRD patterns of G-190 thin film on Pyrex glass and calcined films at 300 and 700°C with powdered $BaTiO_3$ as reference.

crack-free and dense with thickness of about 3 μm after only a single deposition and thermal treatment.

4. CONCLUSIONS

A new glycolate precursor of $BaTiO_3$ was precipitated from an ethylene glycol solution of titanium isopropoxide and monohydrated barium hydroxide and formed the network structure due to nanoscale size and flake-like morphology, resulting in the formation of grease-like gel by incorporation of EG into the network structure. This glycolate precursor was presumed to be layered titania compound intercalated with EG moieties and barium ions from the results of XRD and FTIR data.

Such grease-like gel containing flake-like crystals with stoichiometric composition for Ba and Ti yielded the highly oriented and transparent $BaTiO_3$ thin films of thick coatings in only a single painting and low temperature calcination.

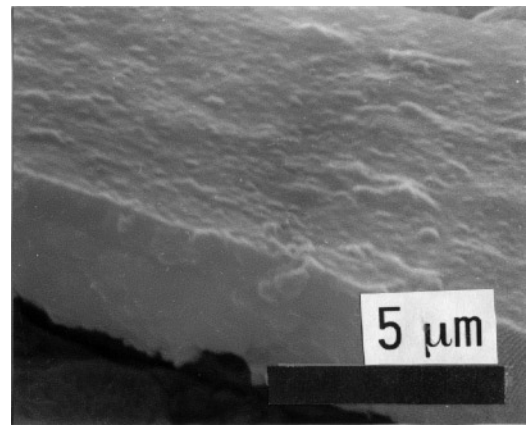

FIG. 7. SEM photograph of G-190 thin film on stainless sheet calcined at 700°C for 30 min.

REFERENCES

1. R. E. Newnham, *Rep. Prog. Phys.* **52,** 123 (1989).
2. L. M. Sheppard, *Am. Ceram. Soc. Bull.* **71,** 85 (1992).
3. Y. C. Yeh and T. Y. Tseng, *J. Mater. Sci. Lett.* **7,** 766 (1988).
4. Z. Zhigang and Z. Gang, *Ferroelectrics* **101,** 43 (1990).
5. T. Ishihara, K. Kometani, Y. Mizuhara, and Y. Takita, *J. Am. Ceram. Soc.* **75,** 613 (1992).
6. P. Li, J. F. Mcdonald, and T.-M. Lu, *Appl. Phys. Lett.* **71,** 5596 (1992).
7. Y. Matsumoto, T. Morikawa, H. Adachi, and J. Hombo, *Mater. Res. Bull.* **27,** 1319 (1992).
8. K. Uchino, N.-Y. Lee, T. Toba, N. Usuki, H. Aburatani, and Y. Ito, *J. Ceram. Soc. Jpn.* **100,** 1091 (1992).
9. K. Y. Chen, L.-L. Lee, and D.-S. Tsai, *J. Mater. Sci. Lett.* **10,** 1000 (1991).
10. M. N. Kamalasanan, S. Chandra, P. C. Joshi, and A. Mansingh, *Appl. Phys. Lett.* **59,** 3547 (1991).
11. N. D. S. Mohallem and M. A. Aegerter, *Mater. Res. Soc. Symp. Proc.* **121,** 515 (1988).
12. K. A. Voloritov, E. V. Orlova, V. I. Ptrovsky, M. I. Yanovskaja, S. A. Ivanov, E. P. Turevskaya, and N. Ya. Turova, *Ferroelectrics* **123,** 261 (1991).
13. C. H. Lee and J. Park, *J. Mater. Sci.* **1,** 219 (1990).
14. D. Hennings and W. Mayr, *J. Solid State Chem.* **26,** 329 (1978).
15. P. K. Gallagher and J. Thomson, Jr., *J. Am. Ceram. Soc.* **48**(12) 644 (1965).
16. A. S. Shaikh and G. M. Vest, *J. Am. Ceram. Soc.* **69,** 682 (1986).
17. M. Rajendran and M. S. Rao, *J. Solid State Chem.* **113,** 239 (1994).
18. J. Fukushima, K. Kodaira, and T. Matsushita, *Am. Ceram. Soc. Bull.* **55,** (1976) 1064.
19. N. D. S. Mohallem and M. A. Aegerter, *in* "Better Ceramics Through Chemistry" (C. J. Brinker, D. R. Clark and D. R. Clark, and D. R. Ulrich, Eds.), Vol. 3, p. 515. Materials Research Society, Pittsburgh, 1988.
20. B. Herrerous, T. L. Barr, and J. Klinowski, *J. Phys. Chem.* **98,** 738 (1994).
21. S. Doeuff, H. Henry, and C. Sanchez, *Mater. Res. Bull.* **25,** 1519 (1990).
22. P. Aranda and E. Ruiz-Hitzky, *Chem. Mater.* **4,** 1395 (1992).
23. M. Inoue, Y. Kondo, and T. Inui, *Inorg. Chem.* **27,** 215 (1988).
24. M. Inoue, Y. Kondo, and T. Inui, *Chem. Lett.* 1421 (1986).
25. S. Kumar, G. L. Messing, and W. White, *J. Am. Ceram. Soc.* **76,** 617 (1993).
26. J. T. Last, *Phys. Rev.* **105,** 1740 (1957).
27. T. Nakamoto, T. Kosaka, S. Omori, and O. Omori, *Ferroelectrics* **37,** 681 (1981).